

Leptoquark patterns unifying neutrino masses, flavor anomalies and the diphoton excess

F. F. Deppisch,¹ S. Kulkarni,² H. Päs,³ and E. Schumacher³

¹*Department of Physics and Astronomy, University College London, London WC1E 6BT, United Kingdom*

²*Institute of High Energy Physics, Austrian Academy of Sciences, Nikolsdorfergasse 18, 1050 Vienna, Austria*

³*Fakultät für Physik, Technische Universität Dortmund, 44221 Dortmund, Germany*

Vector leptoquarks provide an elegant solution to a series of anomalies and at the same time generate naturally light neutrino masses through their mixing with the standard model Higgs boson. We present a simple Froggatt-Nielsen model to accommodate the B physics anomalies R_K and R_D , neutrino masses, and the 750 GeV diphoton excess in one cohesive framework adding only two vector leptoquarks and two singlet scalar fields to the standard model field content.

I. INTRODUCTION

Over the past years several deviations from the standard model (SM) were reported that thus far remain unresolved. Among the most striking are the rare B decay anomalies that manifest themselves in the ratios

$$R_K = \frac{\text{Br}(B \rightarrow K\mu\mu)}{\text{Br}(B \rightarrow Kee)}, \quad R_D = \frac{\text{Br}(B \rightarrow D\tau\nu)}{\text{Br}(B \rightarrow Dl\nu)}, \quad (1)$$

with $l = e, \mu$. The LHCb collaboration reported a 2.6σ deviation from the SM prediction $R_K^{\text{SM}} = 1.0003 \pm 0.0001$, hinting at a violation of lepton universality. The reported result amounts to [1]

$$R_K^{\text{LHCb}} = 0.745 \pm 0.090 \pm 0.036. \quad (2)$$

The ratio $R_{D^{(*)}}$ has been investigated by several experiments, which all see a slight excess over the SM expectation with a combined statistical significance of more than 4σ [2–4],

$$\begin{aligned} R_D^{\text{exp}} &= 0.388 \pm 0.047, & R_{D^*}^{\text{exp}} &= 0.321 \pm 0.021, \\ R_D^{\text{SM}} &= 0.300 \pm 0.010, & R_{D^*}^{\text{SM}} &= 0.252 \pm 0.005. \end{aligned} \quad (3)$$

TeV scale leptoquarks modifying $b \rightarrow sll$ and $b \rightarrow \bar{c}l\nu$ transitions are among the most prominent solutions to the flavor puzzles posed by low-energy precision B physics. Viable candidates to explain the observables R_K and R_D include the scalar leptoquarks $(3, 1)_{2/3}$ and $(3, 3)_{-1/3}$ [5–16], denoted by their $SU(3)_C \otimes SU(2)_L \otimes U(1)_Y$ quantum numbers, and their vector equivalents V_0 and $V_{1/2}$ [17–19]. Attempts have been made using leptoquarks to draw connections beyond B physics to other unexplained phenomena, such as neutrino masses [5, 20–28], neutrinoless double beta ($0\nu\beta\beta$) decay [21, 29], $g-2$ [15, 30, 31], $h \rightarrow \mu\tau$ [31, 32], and even the recently observed diphoton excess near 750 GeV [33, 35]. Vector leptoquarks in particular have been shown to be excellent candidates to explain the latter without the need of introducing many additional fermions [33]. For a very recent review on leptoquark physics, see [34].

In this work we propose viable flavor patterns based on a Froggatt-Nielsen (FN) framework for the vector leptoquarks V_0 and $V_{1/2}$ to accommodate the B physics anomalies R_K and R_D , neutrino masses, and the diphoton excess in one cohesive model. The FN mechanism reproduces the fermion mass hierarchies and quark mixing in excellent agreement with experimental data [36], while the neutrino-leptoquark interactions give rise to the large leptonic mixing angles.

The paper is structured as follows: In Sec. II we review effects of the leptoquarks V_0 and $V_{1/2}$ on rare B decays to address the observed anomalies in R_K and R_D , while accounting for constraints from lepton flavor violation and universality. Considering the results of Sec. II, we cover possible FN charge assignments to generate the required leptoquark couplings in Sec. III. Neutrino mass generation on account of $\Delta L = 2$ Higgs-leptoquark mixing is discussed in Sec. IV, while Sec. V deals with the vector leptoquark resolution to the 750 GeV diphoton excess. We conclude our study in Sec. VI.

II. EXPLAINING RARE B DECAYS WITH VECTOR LEPTOQUARKS

A. R_K

In light of neutrino mass generation we focus only on the vector leptoquarks V_0 and $V_{1/2}$ with electric charge $2/3$, which after Fierz rearrangement [37] induce (axial) vector operators affecting $B \rightarrow Kll$ as shown in Fig. 1(a). Their corresponding quantum numbers under the SM symmetries are given in Table I.

Leptoquark	$(SU(3), SU(2))_{U(1)_Y}$	Q_{EM}	B	L
$V_{1/2}$	$(3, 2)_{1/6}$	$(2/3, -1/3)$	$1/3$	1
V_0	$(3, 1)_{4/3}$	$2/3$	$1/3$	-1

Table I: Quantum numbers of the vector leptoquarks with electric charge $2/3$ that can generate neutrino masses and explain the flavor anomalies.

While scalar leptoquarks can be used to combine R_K with neutrino masses [5], here we focus on their vector counterparts instead to additionally address R_D and the 750 GeV diphoton excess recently observed by CMS and ATLAS [38, 39].

To evade tight constraints from low-energy data [37] we adopt the typical convention [23] that the leptoquark states $V_0 \equiv V_0^L$ and V_0^R , coupling only to lefthanded and righthanded fermions, respectively, are independent particles. Of these states we consider only V_0^L for the remainder of this work, as lefthanded currents are sufficient to explain the SM deviations.

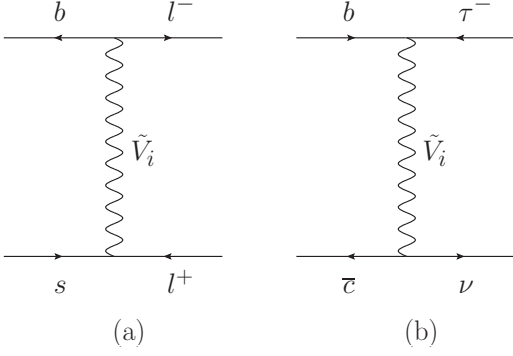


Figure 1: (a) $\bar{b} \rightarrow \bar{s} l^+ l^-$ transition mediated by vector leptoquarks. \tilde{V}_i ($i = 0, 1/2$) denotes the leptoquark mass eigenstates defined in Eq. (36). (b) Charged current $b \rightarrow \bar{c} \tau \nu$ mediated by \tilde{V}_i modifying the ratio R_D .

To quantify effects on R_K we work with an effective Hamiltonian

$$\mathcal{H}_{\text{eff}} = -4 \frac{G_F}{\sqrt{2}} V_{tb} V_{ts}^* \frac{\alpha_e}{4\pi} \sum_i C_i \mathcal{O}_i, \quad (4)$$

where flavor changing $|\Delta B| = |\Delta S| = 1$ quark transitions are accounted for by the operators \mathcal{O}_i and their the Wilson coefficients C_i . Furthermore, G_F denotes the Fermi constant, α_e the electromagnetic fine structure constant, and V_{ud} the Cabibbo-Kobayashi-Maskawa (CKM) matrix elements.

After Fierz rearrangement the V_0 and $V_{1/2}$ leptoquark couplings

$$\mathcal{L}_{\text{LQ}} = \lambda^L \bar{Q} \gamma^\mu L V_{0,\mu} + \lambda^R \bar{u}^c \gamma^\mu L V_{1/2,\mu}^\dagger + \text{h.c.}, \quad (5)$$

give rise to the effective (axial) vector operators

$$\mathcal{O}_9^l = [\bar{s} \gamma^\mu P_L b] [\bar{l} \gamma_\mu l], \quad (6)$$

$$\mathcal{O}_{10}^l = [\bar{s} \gamma^\mu P_L b] [\bar{l} \gamma_\mu \gamma_5 l]. \quad (7)$$

The leptoquark $V_{1/2}$ itself does not couple directly to down-type quarks, but will do so through its mixing with V_0 . However, as leptoquark mixing is required to be small in order to generate naturally light neutrino masses, any effects on R_K or R_D from $V_{1/2}$ are negligible.

A comparison with Eq. (4) yields ($l = e, \mu$),

$$C_9^l = -C_{10}^l = \frac{\pi}{\alpha_e} \frac{\lambda_{sl}^{L*} \lambda_{bl}^L}{V_{tb} V_{ts}^*} \frac{\sqrt{2}}{2m_{V_0}^2 G_F}, \quad (8)$$

where the ql indices denote one element of the matrix λ^L . Consequently, the R_K measurement by LHCb implies at 1σ [6]

$$0.7 \lesssim \text{Re}[X^e - X^\mu] \lesssim 1.5, \quad \text{with } X^l = C_9^l - C_{10}^l = 2C_9^l. \quad (9)$$

Hence, considering only V_0 , we obtain

$$X^e - X^\mu = \frac{\pi}{\sqrt{2} \alpha_e G_F V_{tb} V_{ts}^* m_{V_0}^2} \times \left(\lambda_{se}^{L*} \lambda_{be}^L - \lambda_{s\mu}^{L*} \lambda_{b\mu}^L \right), \quad (10)$$

which is equivalent to

$$\lambda_{se}^{L*} \lambda_{be}^L - \lambda_{s\mu}^{L*} \lambda_{b\mu}^L \simeq (1.8 \pm 0.7) \cdot 10^{-3} \frac{m_{V_0}^2}{\text{TeV}^2}. \quad (11)$$

It has been shown that right handed currents lead to deviations in the double ratio $R_{K^*}/R_K \neq 1$ [7], thereby serving as a potential probe of new physics. However, as stated earlier, any possible effects coming from the $V_{1/2}$ leptoquark state are negligible because of the small leptoquark mixing. Therefore, this framework predicts $R_{K^*} = R_K$.

B. R_D

While a variety of operators contribute to the tree-level process $b \rightarrow \bar{c} l \nu$ depicted in Fig. 1(b), several authors pointed out that the vector operator \mathcal{O}_V gives an excellent fit to the $R_{D^{(*)}}$ data [17–19],

$$\mathcal{O}_V = [\bar{c} \gamma^\mu P_L b] [l \gamma_\mu \nu_l]. \quad (12)$$

In leptoquark UV completions this operator can be provided by both, the $(3, 3)_{2/3}$ and $(3, 1)_{4/3}$ vector leptoquarks V_1 and V_0 . The scalar operators \mathcal{O}_{SL} and \mathcal{O}_{SR} can also explain the data but are incompatible with the measured q^2 spectra available from BaBar and Belle [2, 3]. This disfavors, e.g, generic two-Higgs-doublet model solutions with a charged scalar contribution. In our framework the purely left handed couplings of the leptoquark V_0 generate \mathcal{O}_V with the Wilson coefficient

$$C_{L,l\nu}^{cb} = \frac{1}{2\sqrt{2} G_F V_{cb} m_{V_0}^2} \lambda_{bl}^L \lambda_{c\nu}^{L*}, \quad (13)$$

which translates to the constraint [17, 18]

$$\lambda_{b\tau}^L \lambda_{c\nu_\tau}^{L*} - \lambda_{b\mu}^L \lambda_{c\nu_\mu}^{L*} \simeq (0.18 \pm 0.04) \frac{m_{V_0}^2}{\text{TeV}^2}. \quad (14)$$

Explaining the measurement hence requires a mild hierarchy between the third and the second column of λ^L with $\mathcal{O}(1)$ third generation couplings. Furthermore, any explanation of $R_{D^{(*)}}$ must also accommodate the SM-like branching ratio of $B \rightarrow \tau \bar{\nu}$ [40], requiring further suppression of leptoquark couplings to up quarks.

C. Constraints

The most stringent constraint that leptoquark models aimed at explaining $R_{D^{(*)}}$ have to face, typically comes from nonobservation of the inclusive decay $B \rightarrow X_s \nu \nu$ [16, 19]. As a matter of fact, the $\mathcal{O}(1)$ couplings necessary to explain R_D also affect $b \rightarrow s \nu \nu$ transitions significantly due to $SU(2)$ relations. What makes V_0 such an attractive candidate to explain the rare B decay anomalies is its lack of $\lambda_{d\nu}$ couplings, thereby evading the crucial $B \rightarrow X_s \nu \nu$ constraint. Nevertheless, lepton flavor and universality violating processes involving down-type quarks and charged leptons are still affected by V_0 and have to be taken into consideration. Rare kaon decay data places stringent constraints on the first two quark generations [37],

$$|\lambda_{d\mu}^L \lambda_{s\mu}^{L*}| \lesssim \frac{m_{V_0}^2}{(183 \text{ TeV})^2}. \quad (15)$$

Assuming $m_V \approx 1 \text{ TeV}$, this implies $|\lambda_{d\mu}^L \lambda_{s\mu}^{L*}| \lesssim \epsilon^6$ with $\epsilon \simeq 0.2$. The couplings required to explain R_K and R_D can also be combined to induce flavor violation. These final states are limited for instance by $B^- \rightarrow K^- \mu \tau$ [18, 41],

$$|\lambda_{b\tau}^L \lambda_{s\mu}^L| + |\lambda_{b\mu}^L \lambda_{s\tau}^L| \lesssim \epsilon \frac{m_{V_0}^2}{\text{TeV}^2}. \quad (16)$$

On the other hand, constraints from flavor violating top decays such as $t \rightarrow b \tau \nu_\tau$ are rather weak,

$$|\lambda_{b\tau}^L \lambda_{t\nu_\tau}^L| \lesssim 4.8 \frac{m_{V_0}^2}{\text{TeV}^2}, \quad (17)$$

as opposed to the flavor violating lepton decay $\mu \rightarrow e \gamma$, measured by MEG, which constrains [8, 42]

$$|\lambda_{qe}^L \lambda_{q\mu}^L| \lesssim \frac{m_{V_0}^2}{(34 \text{ TeV})^2}. \quad (18)$$

Thus $|\lambda_{qe}^L \lambda_{q\mu}^L| \lesssim \epsilon^4$ assuming again $m_{V_0} \approx 1 \text{ TeV}$. Summarizing the above constraints, an ideal pattern (excluding possible texture-zero solutions) to account for R_K and R_D and to comply with experimental searches would read

$$\lambda^L \simeq \begin{pmatrix} \epsilon^6 & \epsilon^4 & \epsilon^3 \\ \epsilon^4 & \epsilon^3 & \epsilon \\ \epsilon^3 & \epsilon & 1 \end{pmatrix}. \quad (19)$$

In the following section we study possible $U(1)$ charge assignments to generate such a pattern in a Froggatt-Nielsen framework with two leptoquarks V_0 and $V_{1/2}$.

III. FLAVOR MODEL

To obtain hierarchical leptoquark patterns as required by low energy flavor data, one can embed the particle content in an FN framework that not only addresses the SM flavor anomalies, but also explains the fermion mass hierarchies as well as the CKM mixing [36]. Traditionally, the FN mechanism is implemented with a $U(1)$ shaping symmetry and a scalar singlet field η charged nontrivially under this $U(1)$. The scalar η acquires a VEV v_η at a high scale Λ , suppressing the nonrenormalizable terms of the Yukawa Lagrangian by a factor $\epsilon^n = \left(\frac{v_\eta}{\Lambda}\right)^n \approx 0.2^n$, where n is the sum of the fermion $U(1)_{\text{FN}}$ charges.

Alternatively, one can also employ a discrete Z_N symmetry that in the limit of large N becomes near continuous. This avoids further constraints from anomaly cancellation, or extra gauge bosons arising due to the breaking of the continuous gauge symmetry. Model examples that use Z_N symmetries in this manner can be found in [43–46].

A typical choice of FN charges for the $SU(2)$ doublet fields \bar{Q}_i is $(\bar{Q}_1, \bar{Q}_2, \bar{Q}_3) \sim (3, 2, 0)$, which reproduces the quark mixing angles in good agreement with the Wolfenstein parametrization of the CKM matrix. Since the vector leptoquarks V_0 and $V_{1/2}^\dagger$ couple to \bar{Q} and u , respectively, their patterns will naturally be hierarchical, unlike their scalar leptoquark counterparts S_0^\dagger and $S_{1/2}$ which couple to Q and \bar{d} [5].

Evidently, obtaining the ideal pattern given in Eq. (19) requires the \bar{Q}_i charges $(3, 1, 0)$. Such choice of charges, however, leads to a small Cabibbo angle and large mixing among the second and third quark generations contrary to experimental observations. Bearing a little fine-tuning to explain R_D we will therefore focus on the \bar{Q}_i charges $(3, 2, 0)$.

Besides CKM mixing, another requirement is that the eigenvalues of the fermion mass matrices reflect the observed hierarchies:

$$\begin{aligned} m_u : m_c : m_t &\approx \epsilon^8 : \epsilon^4 : 1, \\ m_d : m_s : m_b &\approx \epsilon^7 : \epsilon^5 : \epsilon^3, \\ m_e : m_\mu : m_\tau &\approx \epsilon^9 : \epsilon^5 : \epsilon^3. \end{aligned} \quad (20)$$

These fermion mass hierarchies fix the $U(1)_{\text{FN}}$ charges of the right handed quark fields. As yet, in the case of the charged leptons the choice remains ambiguous without any further constraint from mixing.

Finally, the interaction $H i \tau_2 V_{1/2}^\mu V_{0\mu}^\dagger$ essential for neutrino masses and mixing, dictates the FN charge assignment $Q(V_0) = Q(V_{1/2})$, provided that the Higgs charge $Q(H) = 0$.

The resulting charge assignments can be expressed in terms of the charge $Q(L_3)$, allowing one to suppress the righthanded couplings λ^R by choosing different integer

values for $Q(L_3) \equiv q_\tau$,

$$\lambda_{V_0}^L \simeq \begin{pmatrix} \epsilon^6 & \epsilon^4 & \epsilon^3 \\ \epsilon^5 & \epsilon^3 & \epsilon^2 \\ \epsilon^3 & \epsilon & 1 \end{pmatrix}, \quad (21)$$

$$\lambda_{V_{1/2}}^R \simeq \begin{pmatrix} \epsilon^{8+2q_\tau} & \epsilon^{6+2q_\tau} & \epsilon^{5+2q_\tau} \\ \epsilon^{5+2q_\tau} & \epsilon^{3+2q_\tau} & \epsilon^{2+2q_\tau} \\ \epsilon^{3+2q_\tau} & \epsilon^{1+2q_\tau} & \epsilon^{2q_\tau} \end{pmatrix}, \quad (22)$$

eg., for $q_\tau = 5$ we obtain

$$\lambda_{V_{1/2}}^R \simeq \begin{pmatrix} \epsilon^{18} & \epsilon^{16} & \epsilon^{15} \\ \epsilon^{15} & \epsilon^{13} & \epsilon^{12} \\ \epsilon^{13} & \epsilon^{11} & \epsilon^{10} \end{pmatrix}. \quad (23)$$

Field	\overline{Q}_1	\overline{Q}_2	\overline{Q}_3	d	s	b	u	c	t
$Q(U(1)_{\text{FN}})$	3	2	0	4	3	3	5	2	0

Field	L_1	L_2	L_3
$Q(U(1)_{\text{FN}})$	$q_\tau + 3$	$q_\tau + 1$	q_τ
Field	e	μ	τ
$Q(U(1)_{\text{FN}})$	$q_\tau - 6$	$q_\tau - 4$	$q_\tau - 2$

Field	V_0	$V_{1/2}^\dagger$	H
$Q(U(1)_{\text{FN}})$	$-q_\tau$	q_τ	0

Table II: Possible $U(1)_{\text{FN}}$ quantum numbers to obtain a flavor model with natural fermion mass hierarchies and approximate CKM mixing in good agreement with experimental data. Choosing $q_\tau = 5$ results in the vector leptoquark patterns discussed in Eq. (23), while larger values of $q_\tau > 5$ will gradually suppress λ^R couplings even further.

The FN charges of Table II yield the following fermion mass matrices up to $\mathcal{O}(1)$ coefficients

$$M_u \simeq \begin{pmatrix} \epsilon^8 & \epsilon^5 & \epsilon^3 \\ \epsilon^7 & \epsilon^4 & \epsilon^2 \\ \epsilon^5 & \epsilon^2 & 1 \end{pmatrix}, \quad M_d \simeq \begin{pmatrix} \epsilon^7 & \epsilon^6 & \epsilon^6 \\ \epsilon^6 & \epsilon^5 & \epsilon^5 \\ \epsilon^4 & \epsilon^3 & \epsilon^3 \end{pmatrix}, \quad (24)$$

$$M_l \simeq \begin{pmatrix} \epsilon^9 & \epsilon^7 & \epsilon^6 \\ \epsilon^7 & \epsilon^5 & \epsilon^4 \\ \epsilon^6 & \epsilon^4 & \epsilon^3 \end{pmatrix}.$$

The fermion mixing matrices that are required to rotate $\lambda^{L,R}$ into the mass basis follow directly from Table II and are approximately given by

$$V_{u,d}^L \simeq \begin{pmatrix} 1 & \epsilon & \epsilon^3 \\ \epsilon & 1 & \epsilon^2 \\ \epsilon^3 & \epsilon^2 & 1 \end{pmatrix}, \quad V_l^{L,R} \simeq \begin{pmatrix} 1 & \epsilon^2 & \epsilon^3 \\ \epsilon^2 & 1 & \epsilon \\ \epsilon^3 & \epsilon & 1 \end{pmatrix}, \quad (25)$$

$$V_u^R \simeq \begin{pmatrix} 1 & \epsilon^3 & \epsilon^5 \\ \epsilon^3 & 1 & \epsilon^2 \\ \epsilon^5 & \epsilon^2 & 1 \end{pmatrix}, \quad V_d^R \simeq \begin{pmatrix} 1 & \epsilon & \epsilon \\ \epsilon & 1 & 1 \\ \epsilon & 1 & 1 \end{pmatrix}. \quad (26)$$

Although the mixing between the second and third lepton generation is enhanced, the FN mechanism is not feasible to explain the large Pontecorvo–Maki–Nakagawa–Sakata (PMNS) mixing angles. Instead, the fundamental difference between the hierarchical CKM and the anarchical PMNS matrix is attributed to neutrino-leptoquark interactions.

The patterns $\lambda^{L,R}$ have to be rotated into their respective mass bases to account for CKM and PMNS mixing. These new matrices are defined as follows:

$$\tilde{\lambda}_{dl}^L = V_d^L \lambda_{V_0}^L V_l^{L\dagger}, \quad \tilde{\lambda}_{u\nu}^L = V_u^L \lambda_{V_0}^L V_\nu^{L\dagger}, \quad (27)$$

$$\tilde{\lambda}_{ul}^R = V_u^R \lambda_{V_{1/2}}^R V_l^{L\dagger}, \quad \tilde{\lambda}_{u\nu}^R = V_u^R \lambda_{V_{1/2}}^R V_\nu^{L\dagger}.$$

Since all relevant mixing matrices of Eqs. (25-26) are approximately diagonal, the general structure of the leptoquark patterns $\lambda^{L,R}$ remains unchanged when rotating from the symmetry into the fermion mass basis. We can henceforth assume $\tilde{\lambda}^{L,R} \simeq \lambda^{L,R}$, with one exception being $\tilde{\lambda}_{u\nu}^L$ that receives large mixing from V_ν^L . The magnitudes of the mixing parameters in V_ν^L can be derived from the experimentally observed PMNS mixing matrix combined with our predictions for V_l^L . From

$$U_{\text{PMNS}} = V_l^{L\dagger} V_\nu^L \Leftrightarrow V_\nu^{L\dagger} = U_{\text{PMNS}}^\dagger V_l^{L\dagger} \quad (28)$$

we infer

$$V_\nu^{L\dagger} \sim \begin{pmatrix} 1 & 1 & \epsilon \\ 1 & 1 & 1 \\ \epsilon & 1 & 1 \end{pmatrix}, \quad \tilde{\lambda}_{u\nu}^L \simeq \begin{pmatrix} \epsilon^4 & \epsilon^3 & \epsilon^3 \\ \epsilon^3 & \epsilon^2 & \epsilon^2 \\ \epsilon & 1 & 1 \end{pmatrix}. \quad (29)$$

All of the obtained patterns are valid only up to $\mathcal{O}(1)$ coefficients, allowing us to estimate the extent of tuning required to accommodate the observables R_K and R_D . Including the $\mathcal{O}(1)$ coefficients, the relevant coupling matrices read

$$\tilde{\lambda}_{dl}^L = \begin{pmatrix} a_{de}\epsilon^6 & a_{d\mu}\epsilon^4 & a_{d\tau}\epsilon^3 \\ a_{se}\epsilon^5 & a_{s\mu}\epsilon^3 & a_{s\tau}\epsilon^2 \\ a_{be}\epsilon^3 & a_{b\mu}\epsilon & a_{b\tau} \end{pmatrix}, \quad (30)$$

$$\tilde{\lambda}_{u\nu}^L = \begin{pmatrix} a_{ue}\epsilon^4 & a_{u\mu}\epsilon^3 & a_{u\tau}\epsilon^3 \\ a_{ce}\epsilon^3 & a_{c\mu}\epsilon^2 & a_{c\tau}\epsilon^2 \\ a_{te}\epsilon & a_{t\mu} & a_{t\tau} \end{pmatrix}. \quad (31)$$

From Eq. (11) we get

$$a_{b\mu}^* a_{s\mu} \simeq -(1.1 \pm 0.4) \frac{m_{V_0}^2}{\text{TeV}^2}, \quad (32)$$

which is a perfect match with R_K data taking $m_{V_0} \approx 1 \text{ TeV}$. On the other hand, the measurement of R_D demands (Eq. (14))

$$a_{b\tau} a_{c\tau}^* - 0.2 \cdot a_{b\mu} a_{c\mu}^* \simeq (4.5 \pm 1.0) \frac{m_{V_0}^2}{\text{TeV}^2}, \quad (33)$$

which requires a little more fine-tuning that can be accommodated easily with couplings mildly larger than 1.

Since the $\lambda_{u\nu}^L$ couplings are slightly enhanced due to the large neutrino mixing, it is suggestive to study up-type flavor transitions to make predictions for D meson decay channels with dineutrino final states. Charm constraints are relatively weak compared to those from the kaon sector, cf. [12].

In our framework, the most promising channel for BSM opportunities is $D^+ \rightarrow \pi^+ \nu \nu$, governed by the couplings $|\lambda_{c\nu}^L \tilde{\lambda}_{u\nu}^L| \approx \epsilon^5$, while predictions for other channels involving charged lepton final states suffer more severe suppression to comply with K physics.

IV. GENERATING NEUTRINO MASSES

As shown in [20, 47], two leptoquarks sharing the same electric charge Q will eventually mix through a coupling with the SM Higgs boson via

$$V(V_i, H) = h_V H i \tau_2 V_{1/2}^\mu V_{0\mu}^\dagger - (m_{V_i}^2 - g_{V_i} H^\dagger H) V_{i,\mu}^\dagger V_i^\mu. \quad (34)$$

The first term, in particular, accounts for the mixing and hence induces neutrino masses if $h_V \neq 0$.

The resulting leptoquark mass eigenstates are a mixture of flavor states with Q_{EM} charge $2/3$ and a distinct $-1/3$ state stemming from $V_{1/2}$,

$$M_{2/3}^2 = \begin{pmatrix} m_{V_0}^2 - g_{V_0} v_{SM}^2 & h_V v_{SM} \\ h_V v_{SM} & m_{V_{1/2}}^2 - g_{V_{1/2}} v_{SM}^2 \end{pmatrix}, \quad (35)$$

$$M_{-1/3}^2 = m_{V_{1/2}}^2 - g_{V_{1/2}} v_{SM}^2.$$

The rotation angle α diagonalizing the $M_{2/3}^2$ matrix is determined by

$$\begin{pmatrix} \tilde{V}_0 \\ \tilde{V}_{1/2} \end{pmatrix} = R \begin{pmatrix} V_0 \\ V_{1/2} \end{pmatrix}, \quad R = \begin{pmatrix} \cos \alpha & -\sin \alpha \\ \sin \alpha & \cos \alpha \end{pmatrix}$$

$$\text{with } \tan 2\alpha = \frac{2h_V v_{SM}}{m_{V_{1/2}}^2 - m_{V_0}^2} = \frac{2h_V v_{SM}}{\Delta m_V^2}, \quad (36)$$

where \tilde{V}_i denotes the leptoquark mass eigenstates.

The dimensionful parameter h_V cannot be arbitrarily large, but is in fact limited by the condition of positive leptoquark masses and the perturbativity of the theory to

$$h_V \leq m'_{V_0} m'_{V_{1/2}} / v_{SM}$$

$$\text{with } m'_{V_i} \equiv \sqrt{m_{V_i}^2 - g_{V_i} v_{SM}^2}. \quad (37)$$

Since two leptoquarks with couplings to up-type quarks and neutrinos are present, their $\Delta L = 2$ mixing induced by the Higgs boson interaction $h_V H i \tau_2 V_{1/2}^\mu V_{0\mu}^\dagger$ generates Majorana neutrino masses at one-loop level as depicted in Fig. 2.

The magnitude of the neutrino mass depends on the leptoquark mixing, governed by the dimensionful parameter

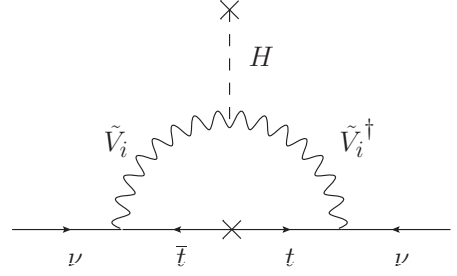


Figure 2: One-loop Majorana neutrino mass generated by Higgs-leptoquark mixing.

h_V , and on the leptoquark couplings $\lambda^{L,R}$. Explicitly, the contribution to the Majorana neutrino mass from $V_{0,\mu}$ and $V_{1/2,\mu}$ is given by

$$M_{ii'}^\nu = \frac{3}{16\pi^2} \sum_{j=1,2} \sum_{k=u,c,t} m_k B_0(0, m_k^2, m_{V_j}^2) R_{j1} R_{j2} \times [\lambda_{ki}^R \lambda_{ki'}^L + \lambda_{ki'}^R \lambda_{ki}^L], \quad (38)$$

herein is m_{V_j} the mass of the leptoquark V_j , m_k the quark mass and R_{jl} the mixing matrix diagonalizing the leptoquark mass matrix, while B_0 denotes the finite part of the Passarino-Veltman function

$$B_0(0, m_k^2, m_{V_j}^2) = \frac{m_k^2 \log(m_k^2) - m_{V_j}^2 \log(m_{V_j}^2)}{m_k^2 - m_{V_j}^2}. \quad (39)$$

Using the leptoquark patterns discussed in Eqs. (21-23), we can estimate the absolute neutrino mass scale generated by the leptoquark couplings. Since the patterns are strongly hierarchical in terms of quark families, we need only consider the dominating top quark contribution to $M_{ii'}^\nu$. Hence, we obtain

$$M_{ii'}^\nu \approx \underbrace{\frac{3}{32\pi^2} m_t \sin 2\alpha \Delta B_0}_{\equiv a} [\lambda_{ti}^R \lambda_{ti'}^L + \lambda_{ti'}^R \lambda_{ti}^L],$$

$$\Delta B_0 \equiv B_0(0, m_t^2, m_{V_{1/2}}^2) - B_0(0, m_t^2, m_{V_0}^2), \quad (40)$$

and the neutrino mass eigenstates

$$m_1^\nu = 0, \quad (41)$$

$$\frac{m_{2(3)}^\nu}{a} = \sum_i \lambda_{ti}^L \lambda_{ti(+)}^R \sqrt{\sum_i (\lambda_{ti}^L)^2 \sum_i (\lambda_{ti}^R)^2} \quad (42)$$

with $i = e, \mu, \tau$. Note that one eigenvalue is exactly zero if either only down-type or up-type quarks generate neutrino masses. Hence, the model predicts a normal neutrino mass hierarchy with a small effective Majorana mass relevant for $0\nu\beta\beta$.

Inserting Eqs. (21-23) yields

$$M_{ii'}^\nu \propto a \cdot \begin{pmatrix} \epsilon^{16} & \epsilon^{14} & \epsilon^{13} \\ \epsilon^{14} & \epsilon^{12} & \epsilon^{11} \\ \epsilon^{13} & \epsilon^{11} & \epsilon^{10} \end{pmatrix}, \quad \text{and } m_3^\nu \sim a \cdot \epsilon^{10}. \quad (43)$$

Therefore, the factor a must be sufficiently small to push the neutrino mass scale below eV, which is achieved by virtue of small leptoquark mixing. In the limit of small a the parameter a can be approximated as

$$a \approx \frac{3}{16\pi^2} m_t \frac{h_V v_{\text{SM}}}{\Delta m_V^2} \log \left[\frac{m_{V_{1/2}}^2}{m_{V_0}^2} \right], \quad (44)$$

implying

$$\frac{h_V v_{\text{SM}}}{\Delta m_V^2} \log \left[\frac{m_{V_{1/2}}^2}{m_{V_0}^2} \right] \lesssim 0.9 \times 10^{-3} \quad (45)$$

to make neutrino masses sufficiently light. The smallness of a can be attributed to the smallness of the dimensionful coupling h_V or a large mass splitting Δm_V^2 of the contributing leptoquarks. Possible solutions of Eq. (45) are depicted in Fig. 3 for different powers of $\lambda^R \sim \epsilon^8, \epsilon^{10}$, and ϵ^{12} . In Fig. 4 we plot m_ν' in terms of $m_{V_{1/2}}$ for $\lambda^R \sim \epsilon^{10}$ and $h_V = 0.1, 0.5$, and 1 TeV, showing that light neutrino masses favor a large leptoquark mass splitting with natural values of h_V .

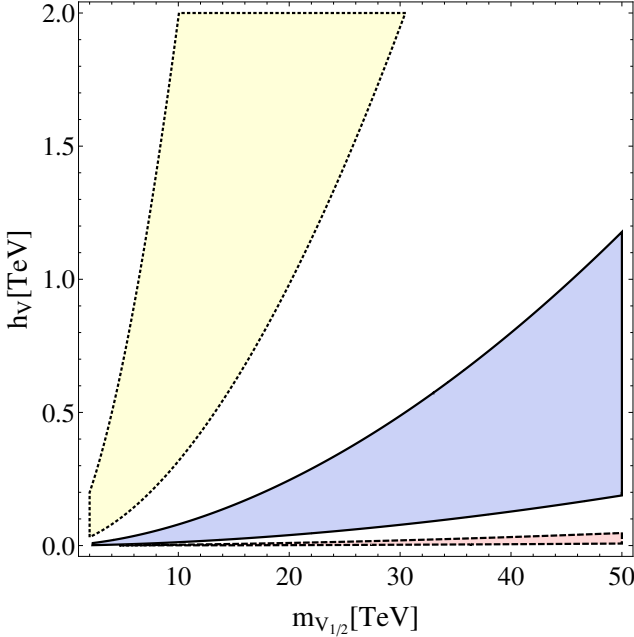


Figure 3: Allowed regions of the trilinear leptoquark-Higgs coupling h_V and $m_{V_{1/2}}$ requiring that the largest neutrino mass eigenstate $m_\nu \lesssim 0.3 \text{ eV}$ and $m_{V_0} \simeq 1 \text{ TeV}$. The three distinct regions correspond to different powers of the dominating coupling $\lambda_{\nu\nu}^R \simeq \epsilon^8$ (red, dashed), ϵ^{10} (blue, solid) and ϵ^{12} (yellow, dotted).

Since one neutrino mass eigenstate is exactly zero, one can solve the eigenvalue equation $M_\nu v_0 = 0$ with

$$v_0^T = \frac{(1, -w, w')}{\sqrt{1 + w^2 + w'^2}} \quad (46)$$

to obtain analytical expressions for the neutrino mixing angles as a function of the leptoquark couplings $\lambda_{\nu\nu}^{L,R}$,

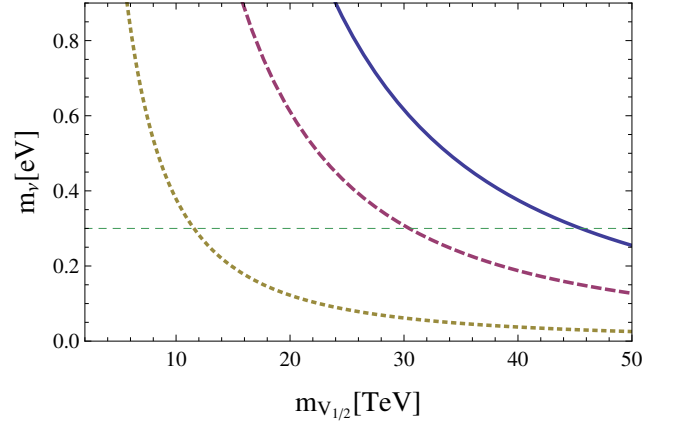


Figure 4: Heaviest neutrino mass eigenstate as a function of $m_{V_{1/2}}$ for $m_{V_0} = 1 \text{ TeV}$, $\lambda_{\nu\nu}^R \simeq \epsilon^{10}$ and $h_V = 1 \text{ TeV}$ (blue, solid), 0.5 TeV (red, dashed), 0.1 TeV (yellow, dotted).

assuming the charged leptons are approximately diagonal [23]. It is

$$w = \frac{\lambda_{t\tau}^R \lambda_{te}^L - \lambda_{te}^R \lambda_{t\tau}^L}{\lambda_{t\tau}^R \lambda_{t\mu}^L - \lambda_{t\mu}^R \lambda_{t\tau}^L} \approx t_{12} \frac{c_{23}}{c_{13}} + t_{13} s_{23}, \quad (47)$$

$$w' = \frac{\lambda_{t\mu}^R \lambda_{te}^L - \lambda_{te}^R \lambda_{t\mu}^L}{\lambda_{t\tau}^R \lambda_{t\mu}^L - \lambda_{t\mu}^R \lambda_{t\tau}^L} \approx t_{12} \frac{s_{23}}{c_{13}} - t_{13} c_{23}, \quad (48)$$

where, $s_{23} = \sin \theta_{23}$ etc. with the PMNS angles $\theta_{12}, \theta_{23}, \theta_{13}$. Hence, to explain large PMNS mixing w and w' both should be nonzero and sizable. By evaluating w and w' for Eqs. (21-23) we find that their values depend heavily on the undetermined $\mathcal{O}(1)$ FN parameters

$$w = \frac{y_{31} - y_{13}}{y_{32} - y_{23}} \epsilon^2, \quad w' = \frac{y_{21} - y_{12}}{y_{32} - y_{23}} \epsilon^3, \quad (49)$$

where y_{ij} denote products of $\mathcal{O}(1)$ coefficients from $\lambda^{L,R}$. Because of possible cancellation in the denominator, w and w' can oscillate quickly with small changes of the $\mathcal{O}(1)$ parameters, explaining also large neutrino mixing easily by permitting some extent of tuning.

With many free $\mathcal{O}(1)$ FN parameters to match to only five physical observables ($\Delta m_{\text{atm}}^2, \Delta m_{\text{sol}}^2, \theta_{12}, \theta_{13}, \theta_{23}$), the system is underconstrained and has many viable solutions. On condition that all coefficients in Eq. (24) are approximately $\mathcal{O}(1)$, the benchmark point

$$\begin{aligned} \lambda_{te}^L &\approx 5.1 \epsilon^3, & \lambda_{te}^R &\approx 3.0 \epsilon^{13}, \\ \lambda_{t\mu}^L &\approx 1.4 \epsilon, & \lambda_{t\mu}^R &\approx 2.1 \epsilon^{11}, \\ \lambda_{t\tau}^L &\approx 0.2, & \lambda_{t\tau}^R &\approx -0.8 \epsilon^{10}, \end{aligned} \quad (50)$$

provides an excellent fit to neutrino oscillation data, yielding

$$\begin{aligned} \Delta m_{\text{atm}}^2 &= 2.5 \times 10^{-3} \text{ eV}^2, & \Delta m_{\text{sol}}^2 &= 7.6 \times 10^{-5} \text{ eV}^2, \\ \theta_{12} &= 33.3^\circ, & \theta_{13} &= 8.5^\circ, & \theta_{23} &= 42.0^\circ. \end{aligned} \quad (51)$$

Further limits on $\Delta L = 2$ lepton number violating leptoquark couplings also arise from $0\nu\beta\beta$ experiments, which

can be even more stringent than LHC searches [21, 29]. The mixing of V_0 and $V_{1/2}$ induced by the SM Higgs boson generates the operator [29]

$$\lambda_{de}^L \lambda_{uv}^R \frac{h_V v_{\text{SM}}}{m_{V_{1/2}}^2 m_{V_0}^2} [\bar{v} P_R e^c] [\bar{u} P_R d]. \quad (52)$$

Given the strong suppression of first generation couplings combined with the extra suppression of λ^R , the $0\nu\beta\beta$ bound is negligible in this framework. By contrast, scalar leptoquarks with inverse hierarchical patterns can reduce the $0\nu\beta\beta$ half-life considerably, allowing for an observation of the $0\nu\beta\beta$ decay in the near future [5].

V. 750 GeV DIPHOTON EXCESS

Recently, the ATLAS and CMS collaborations reported an excess in the diphoton spectrum near 750 GeV with 3.9σ and 2.6σ local significance [38, 39]. The signal hints at a potential resonance with spin 0 or 2 and strongly enhanced branching ratios into gluons and photons.

A plethora of explanations has been considered by various authors since the announcement of the excess, among them also leptoquark mediators. While pure scalar leptoquark solutions face difficulties regarding unitarity, vector leptoquarks can explain the signal rather elegantly thanks to a sizable loop factor. The beauty of the vector leptoquark solution is that it does not come with numerous exotic fermions to artificially enhance the diphoton decay mode.

The vector leptoquarks in our model can interact with the scalar resonance χ through the hypothetical interaction

$$\mathcal{L}_{V\chi} = \kappa_{V_i} \chi V_{\mu,i}^\dagger V_i^\mu + \text{h.c.}, \quad (53)$$

where $i = 0, \frac{1}{2}$. κ_{V_i} is a dimensionful parameter whose scale thus far is undetermined, however bounded from above by unitarity constraints. The scale where the theory breaks down can be roughly inferred from elastic $V_{i,\mu} V^{i,\mu} \rightarrow V_{i,\mu} V^{i,\mu}$ scattering, given by $\sqrt{s} \sim 4\sqrt{\pi} m_{V_i}^2 / |\kappa_{V_i}|$ [33]. In the following we will assume natural $\mathcal{O}(1 \text{ TeV})$ values for κ_{V_i} to comply with perturbative unitarity.

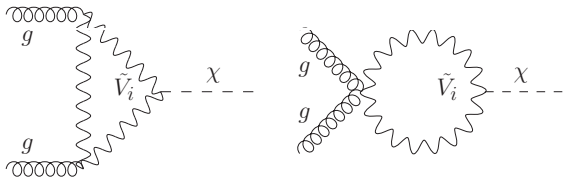


Figure 5: Dominating diagrams contributing to $\sigma(pp \rightarrow \chi)$.

The total cross section σ is a product of the χ production and its subsequent decay rate into two photons. χ

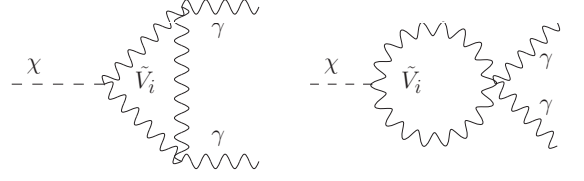


Figure 6: Diagrams contributing to $\Gamma(\chi \rightarrow \gamma\gamma)$.

production from $q\bar{q}$ initial states is possible, however, strongly suppressed either by small leptoquark couplings (cf. Eqs. (21-23)) or small values of the parton distribution functions at $\sqrt{s} = 13 \text{ TeV}$ [53]. The only partly competitive channel in terms of luminosity, $d\bar{d} \rightarrow \chi$, is additionally suppressed compared to gluon fusion by a factor of $|\lambda_{d\tau}^L|^2 = \epsilon^6$ due to the FN symmetry. Hence, assuming that χ is predominantly produced via gluon fusion we obtain [48]

$$\sigma(pp \rightarrow \chi \rightarrow \gamma\gamma) = \frac{\pi^2}{8s} \frac{\Gamma(\chi \rightarrow \gamma\gamma)}{\Gamma_{\text{tot}}} \times \frac{\Gamma(\chi \rightarrow gg)}{m_\chi} f_{gg} \left(\frac{m_\chi^2}{s} \right) \quad (54)$$

with

$$\Gamma(\chi \rightarrow gg) = \frac{\alpha_s^2 m_\chi K^{gg}}{128\pi^3} \left| \sum_i \frac{\kappa_{V_i} A_1(\tau_{V_i})}{m_{V_i}} \right|^2, \quad (55)$$

$$\Gamma(\chi \rightarrow \gamma\gamma) = \frac{\alpha_e^2 m_\chi}{256\pi^3} \left| \sum_i \frac{\kappa_{V_i} N_c Q_{V_i}^2 A_1(\tau_{V_i})}{m_{V_i}} \right|^2, \quad (56)$$

where $i = 0, \frac{1}{2}$. Henceforth, we will denote $\sigma(pp \rightarrow \chi \rightarrow \gamma\gamma)$ by $\sigma_{\gamma\gamma}$, $\Gamma(\chi \rightarrow gg)$ by Γ_{gg} and $\Gamma(\chi \rightarrow \gamma\gamma)$ by $\Gamma_{\gamma\gamma}$. We furthermore approximate $\Gamma_{\text{tot}} \approx \Gamma_{gg}$. K^{gg} accounts for higher order QCD corrections, $N_c = 3$ for the vector leptoquarks running in the loop and α_s is the strong coupling constant. $A_1(\tau)$ denotes a loop factor for a spin 1 particle given by [49]

$$A_1(\tau) = \frac{1}{\tau^2} [2\tau^2 + 3\tau + 3(2\tau - 1) \arcsin^2 \sqrt{\tau}], \quad (57)$$

and $\tau_{V_i} = m_\chi^2 / (4m_{V_i}^2) < 1$. For completeness, the spin 0 and spin 1/2 loop factors read

$$A_0(\tau) = -\frac{1}{\tau^2} [\tau - \arcsin^2 \sqrt{\tau}], \quad (58)$$

$$A_{1/2}(\tau) = \frac{2}{\tau^2} [\tau + (\tau - 1) \arcsin^2 \sqrt{\tau}], \quad (59)$$

respectively. $A_1(\tau)$ acquires large values for vector leptoquarks compared to scalar particles. Assuming masses ranging from $\sim 0.8 \text{ TeV}$ to 50 TeV , the loop factors remain near constant and

$$\frac{A_1(\tau)}{A_0(\tau)} \approx 20, \quad \frac{A_1(\tau)}{A_{1/2}(\tau)} \approx 5, \quad (60)$$

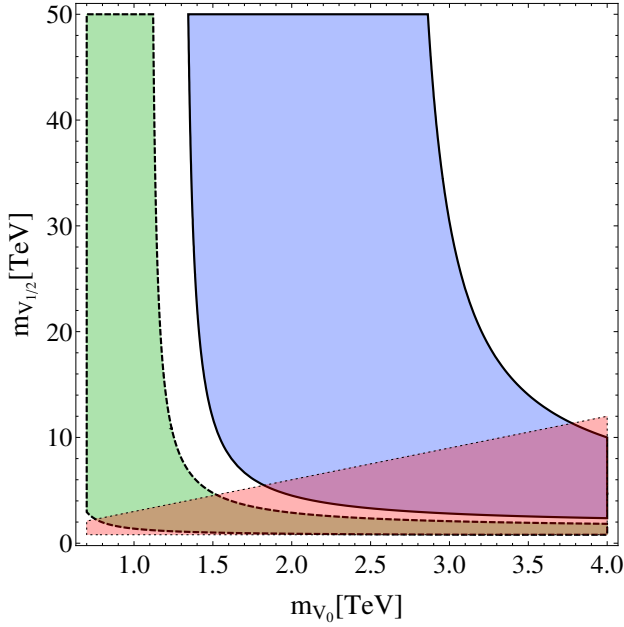


Figure 7: Parameter regions yielding $\sigma_{\gamma\gamma} \in (3, 13)$ fb as measured by ATLAS and CMS. $\sigma_{\gamma\gamma}$ as a function of the lepto-quark masses m_{V_0} and $m_{V_{1/2}}$ for different values of the dimensionful couplings $\kappa_{V_i} = 2.5$ TeV (blue, solid) and 1 TeV (green, dashed). The WW , ZZ and $Z\gamma$ exclusion limits are superimposed in red.

in the relevant mass region.

The gluon luminosity function f_{gg} , evaluated at $\sqrt{s} = 13$ TeV using MSTW2008 [50] leads to

$$f_{gg} = \int_{\frac{m_\chi^2}{s}}^1 f_g(x) f_g\left(\frac{m_\chi^2}{xs}\right) \frac{dx}{x} = 2141.7, \quad (61)$$

where f_g is the gluon distribution function. Depending on the dimensionful couplings κ_{V_i} , typical values of Γ_{gg}/m_χ and $\Gamma_{\gamma\gamma}/m_\chi$ are $\mathcal{O}(10^{-4})$ and $\mathcal{O}(10^{-6})$, respectively. In our setup, at the benchmark point $\kappa_{V_0} = \kappa_{V_{1/2}} = m_{V_0} = 1$ TeV and $m_{V_{1/2}} = 20$ TeV we have

$$\frac{\Gamma_{gg}}{m_\chi} \simeq 2 \cdot 10^{-4}, \quad \frac{\Gamma_{\gamma\gamma}}{m_\chi} \simeq 8 \cdot 10^{-7}, \quad \sigma_{\gamma\gamma} \simeq 4 \text{ fb}. \quad (62)$$

Therefore, the dijet estimated cross section at 13 TeV is 4 pb, leading to a cross section $\simeq 0.8$ pb at 8 TeV. Currently the ATLAS and CMS collaborations do not provide dijet limits at $\sqrt{s} = 13$ TeV for resonance masses below 1 TeV. The $\sqrt{s} = 8$ TeV ATLAS and CMS analyses presented in [51, 52] set a limit of $\sigma_{jj} < 1$ pb for a 1 TeV resonance coupling dominantly to gg . For a mass of 750 GeV the limit shown by ATLAS is of the order of 10 pb. Hence within the interesting region of parameter space considered here, the dijet limits are satisfied.

As V_0 and $V_{1/2}$ carry hypercharge, they necessarily decay via $\chi \rightarrow Z\gamma$ and $\chi \rightarrow ZZ$. Limits on these final states from experimental collaborations already exist. Here we

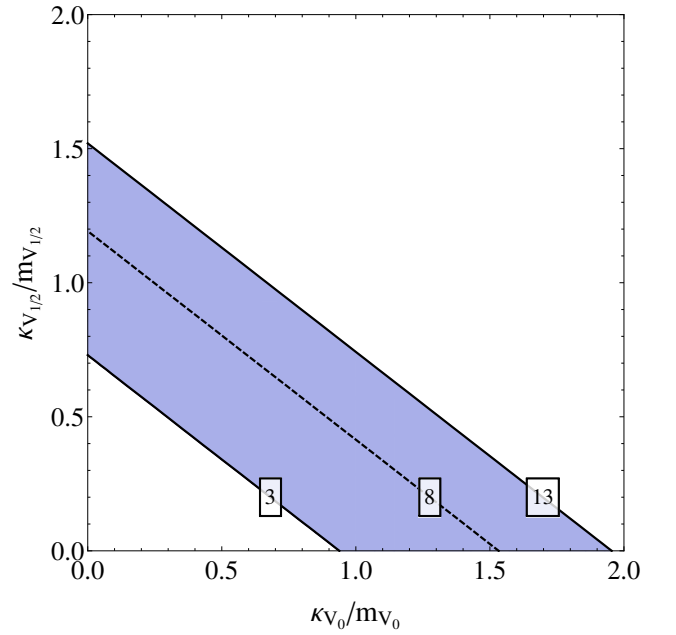


Figure 8: Parameter regions yielding $\sigma_{\gamma\gamma} \in (3, 13)$ fb as measured by ATLAS and CMS. $\sigma_{\gamma\gamma}$ as a function of the effective parameters κ_{V_i}/m_{V_i} . The contours denote values of constant $\sigma_{\gamma\gamma}$ in fb.

take a rather simplistic viewpoint and assess the viability of our scenario without explicitly calculating the cross sections for $Z\gamma, ZZ$ final states. This can be done by estimating the ratios of χ partial widths. The partial widths $\chi \rightarrow Z\gamma$ and $\chi \rightarrow ZZ$ are suppressed by $2 \tan^2 \theta_W$ and $\tan^4 \theta_W$, respectively, compared to $\Gamma_{\gamma\gamma}$ and existing bounds on these channels can be easily evaded. More importantly, $V_{1/2}$ is an $SU(2)$ doublet with enhanced rates $\Gamma_{Z\gamma}/\Gamma_{\gamma\gamma} \approx 2/\tan^2 \theta_W$, $\Gamma_{ZZ}/\Gamma_{\gamma\gamma} \approx 1/\tan^4 \theta_W$. In addition, the decay to two W bosons will be possible as well with a strongly enhanced rate $\Gamma_{WW}/\Gamma_{\gamma\gamma} \approx 2/\sin^2 \theta_W$. In order to sufficiently suppress these rates below their experimental limits, it is necessary that $V_{1/2}$ is heavier than V_0 by at least a factor of 2 to 3 [53]. We use this limit on the mass of $V_{1/2}$ in order to quantify the impact of diboson final state limits in our analysis.

The width of χ is dominated by the decay to gluons and it is typically small, $\Gamma_{\text{tot}} \approx \Gamma_{gg} \approx 0.3$ GeV. We make no attempt to explain a potentially large width as suggested by ATLAS within this setup.

In the following we determine the allowed parameter ranges of κ_{V_i} and m_{V_i} to reproduce the total cross sections measured by ATLAS and CMS in the diphoton channel near 750 GeV

$$\sigma_{\text{ATLAS}} = (10 \pm 3) \text{ fb}, \quad \sigma_{\text{CMS}} = (6 \pm 3) \text{ fb}. \quad (63)$$

Taking into account that $m_{V_0} \sim 1$ TeV is needed to reproduce the R_K and R_D data, we obtain the allowed parameter regions displayed in Figs. 7 and 8 as a function of the dimensionful couplings κ_{V_i} and the lepto-quark masses m_{V_i} , respectively. The parameter space

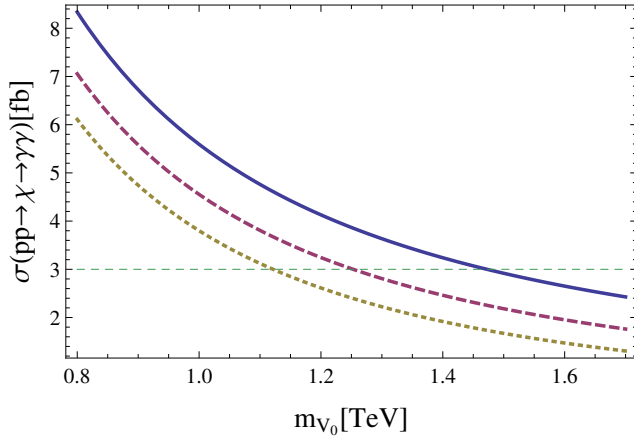


Figure 9: $\sigma(pp \rightarrow \chi \rightarrow \gamma\gamma)$ as a function of m_{V_0} for $m_{V_{1/2}} = 5$ TeV (blue, solid), 10 TeV (red, dashed), 50 TeV (yellow, dotted) with $\kappa_{V_i} = 1$ TeV. The horizontal, dashed lines correspond to the lower limit given by the ATLAS and CMS diphoton measurements.

favouring the diphoton cross section opens up notably if the second leptoquark is much heavier, yielding a large Δm_V^2 that is also favored by neutrino mass generation. Fig. 7 represents the $\sigma_{\gamma\gamma}$ in the range of 3 – 13 fb, for two different values of dimensionful couplings κ_{V_i} . The parameter space excluded by $WW, ZZ, Z\gamma$ final states is depicted in red. This constraint is derived using simple ratios of partial widths as discussed before, we impose $m_{V_{1/2}}/m_{V_0} > 3$. In the parameter space satisfying $\sigma_{\gamma\gamma}$ between 3–13 fb, $m_{V_0} > 1.5$ TeV is excluded by $WW, ZZ, Z\gamma$ constraints for $\kappa_{V_i} = 1$ TeV. For $\kappa_{V_i} = 2.5$ TeV, the diphoton cross section requires a minimum $m_{V_0} \approx 1.4$ TeV, while the $WW, ZZ, Z\gamma$ constraints rule out all $m_{V_0} > 3.8$ TeV.

In Fig. 8 we depict $\sigma_{\gamma\gamma}$ as a function of κ_{V_i}/m_{V_i} . It can be seen that $\sigma_{\gamma\gamma}$ quickly becomes too large if both dimensionful couplings κ_{V_i} are of the order of the leptoquark masses. We fix the loop factor $A_1(\tau) \sim 7$, after explicitly verifying that $A_1(\tau)$ varies by 3% in the relevant region of parameter space. The residual dependence on the masses from the loop function is hence small and is ignored. As $\kappa_{V_0}/m_{V_0}, \kappa_{V_{1/2}}/m_{V_{1/2}}$ increases, the corresponding diphoton cross section increases and the observed excess can be explained with, e.g., $\kappa_{V_0}/m_{V_0} \approx 1$ and $\kappa_{V_{1/2}}/m_{V_{1/2}} < 0.8$.

In Fig. 9 we show the behavior of $\sigma_{\gamma\gamma}$ in terms of m_{V_0} for different choices of $m_{V_{1/2}}$ while keeping $\kappa_{V_i} = 1$ TeV fixed. The diphoton cross section decreases with large leptoquark masses and a mass $m_{V_0} \approx 1$ TeV is preferred in good agreement with the input from rare B decays. For a given value of $m_{V_{1/2}}$, the diphoton cross section requirement yields an upper bound on m_{V_0} . In the case $m_{V_{1/2}} = 50$ TeV, $m_{V_0} > 1.1$ TeV yields a too low diphoton cross section, while $m_{V_{1/2}} = 5$ TeV requires $m_{V_0} < 1.5$ TeV.

The benchmark point $m_{V_0} = 1$ TeV, $m_{V_{1/2}} = 50$ TeV,

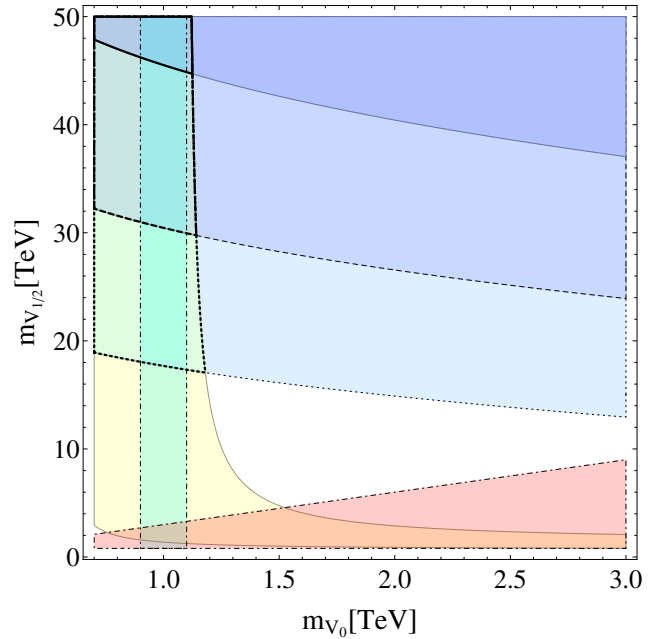


Figure 10: Fit results of the 750 GeV diphoton excess (yellow) superimposed with constraints from neutrino mass generation (blue) in the leptoquark parameter space for $\kappa_{V_i} = 1$ TeV and $h_V = 0.2$ TeV (dotted), 0.5 TeV (dashed), 1 TeV (solid). The cyan overlay (dotted/dashed) denotes regions favored by low energy B physics. The constraints favor a combination of a light V_0 and a heavy $V_{1/2}$ with $m_{V_0} \approx 1$ TeV and $m_{V_{1/2}} \gtrsim 20$ TeV, depending on the scale of the trilinear couplings κ_{V_i} and h_V . The parameter space excluded by $WW, ZZ, Z\gamma$ constraints is depicted in red.

$\kappa_{V_i} = 1$ TeV yields $\sigma \approx 5.6$ fb in good agreement with Eq. (63). Intriguingly, the combined results of neutrino mass generation and the 750 GeV diphoton excess point to a similar region in the parameter space of leptoquark masses. As shown in Fig. 10 the overlay of all constraints points at a light leptoquark $m_{V_0} \approx 1$ TeV together with a heavy $m_{V_{1/2}} \gtrsim 20$ TeV, depending on the size of the trilinear couplings κ_{V_i} and h_V .

VI. CONCLUSION

The same leptoquarks that explain the recently observed anomalies in rare B meson decays can generate naturally small Majorana neutrino masses at one-loop level through a $\Delta L = 2$ Higgs coupling.

By proposing a simple framework based on an FN mechanism, we have shown that addressing several issues at the same time is entirely feasible and need not be overly fine-tuned. The total additional field content necessary to explain R_K, R_D , the 750 GeV excess and neutrino masses and mixing, includes no more than two vector leptoquarks and two SM singlet scalars. Only one additional symmetry is required to shape the fermion mass matrices and leptoquark couplings to comply with exper-

imental data.

Our analysis shows that two leptoquarks with masses $m_{V_0} \approx 1 \text{ TeV}$ and $m_{V_{1/2}} \gtrsim 30 \text{ TeV}$ are favored to explain the diphoton excess and the lightness of neutrino masses. Furthermore, the model predicts dominant third generation leptoquark decays, mostly into $b\tau$ final states, and an enhanced $D^+ \rightarrow \pi^+ \nu \nu$ rate for indirect leptoquark searches. On the other hand, the already tightly constrained inclusive decay $B \rightarrow X_s \nu \nu$ remains SM like.

VII. ACKNOWLEDGMENT

HP thanks A. Crivellin for helpful discussions. SK is supported by the ‘New Frontiers’ program of the Austrian Academy of Sciences.

-
- [1] R. Aaij *et al.* [LHCb Collaboration], Phys. Rev. Lett. **113**, 151601 (2014) doi:10.1103/PhysRevLett.113.151601 [arXiv:1406.6482 [hep-ex]].
 - [2] J. P. Lees *et al.* [BaBar Collaboration], Phys. Rev. D **88**, no. 7, 072012 (2013) doi:10.1103/PhysRevD.88.072012 [arXiv:1303.0571 [hep-ex]].
 - [3] M. Huschle *et al.* [Belle Collaboration], Phys. Rev. D **92**, no. 7, 072014 (2015) doi:10.1103/PhysRevD.92.072014 [arXiv:1507.03233 [hep-ex]].
 - [4] R. Aaij *et al.* [LHCb Collaboration], Phys. Rev. Lett. **115**, no. 11, 111803 (2015) [Phys. Rev. Lett. **115**, no. 15, 159901 (2015)] doi:10.1103/PhysRevLett.115.159901, 10.1103/PhysRevLett.115.111803 [arXiv:1506.08614 [hep-ex]].
 - [5] H. Päs and E. Schumacher, Phys. Rev. D **92**, no. 11, 114025 (2015) doi:10.1103/PhysRevD.92.114025 [arXiv:1510.08757 [hep-ph]].
 - [6] G. Hiller and M. Schmaltz, Phys. Rev. D **90**, 054014 (2014) doi:10.1103/PhysRevD.90.054014 [arXiv:1408.1627 [hep-ph]].
 - [7] G. Hiller and M. Schmaltz, JHEP **1502**, 055 (2015) doi:10.1007/JHEP02(2015)055 [arXiv:1411.4773 [hep-ph]].
 - [8] I. de Medeiros Varzielas and G. Hiller, JHEP **1506**, 072 (2015) doi:10.1007/JHEP06(2015)072 [arXiv:1503.01084 [hep-ph]].
 - [9] S. Sahoo and R. Mohanta, Phys. Rev. D **93**, no. 3, 034018 (2016) doi:10.1103/PhysRevD.93.034018 [arXiv:1507.02070 [hep-ph]].
 - [10] S. Sahoo and R. Mohanta, New J. Phys. **18**, no. 1, 013032 (2016) doi:10.1088/1367-2630/18/1/013032 [arXiv:1509.06248 [hep-ph]].
 - [11] R. Alonso, B. Grinstein and J. M. Camalich, JHEP **1510**, 184 (2015) doi:10.1007/JHEP10(2015)184 [arXiv:1505.05164 [hep-ph]].
 - [12] S. de Boer and G. Hiller, arXiv:1510.00311 [hep-ph].
 - [13] D. Bečirević, S. Fajfer and N. Košnik, Phys. Rev. D **92**, no. 1, 014016 (2015) doi:10.1103/PhysRevD.92.014016 [arXiv:1503.09024 [hep-ph]].
 - [14] B. Gripaios, M. Nardecchia and S. A. Renner, JHEP **1505**, 006 (2015) doi:10.1007/JHEP05(2015)006 [arXiv:1412.1791 [hep-ph]].
 - [15] M. Bauer and M. Neubert, arXiv:1511.01900 [hep-ph].
 - [16] Y. Sakaki, M. Tanaka, A. Tayduganov and R. Watanabe, Phys. Rev. D **88**, no. 9, 094012 (2013) doi:10.1103/PhysRevD.88.094012 [arXiv:1309.0301 [hep-ph]].
 - [17] M. Freytsis, Z. Ligeti and J. T. Ruderman, Phys. Rev. D **92**, no. 5, 054018 (2015) doi:10.1103/PhysRevD.92.054018 [arXiv:1506.08896 [hep-ph]].
 - [18] S. Fajfer and N. Košnik, Phys. Lett. B **755**, 270 (2016) doi:10.1016/j.physletb.2016.02.018 [arXiv:1511.06024 [hep-ph]].
 - [19] L. Calibbi, A. Crivellin and T. Ota, Phys. Rev. Lett. **115**, 181801 (2015) doi:10.1103/PhysRevLett.115.181801 [arXiv:1506.02661 [hep-ph]].
 - [20] M. Hirsch, H. V. Klapdor-Kleingrothaus and S. G. Kovalenko, Phys. Lett. B **378**, 17 (1996) doi:10.1016/0370-2693(96)00419-4 [hep-ph/9602305].
 - [21] J. C. Helo, M. Hirsch, H. Päs and S. G. Kovalenko, Phys. Rev. D **88**, 073011 (2013) doi:10.1103/PhysRevD.88.073011 [arXiv:1307.4849 [hep-ph]].
 - [22] U. Mahanta, Phys. Rev. D **62**, 073009 (2000) doi:10.1103/PhysRevD.62.073009 [hep-ph/9909518].
 - [23] D. Aristizabal Sierra, M. Hirsch and S. G. Kovalenko, Phys. Rev. D **77**, 055011 (2008) doi:10.1103/PhysRevD.77.055011 [arXiv:0710.5699 [hep-ph]].
 - [24] K. S. Babu and J. Julio, Nucl. Phys. B **841**, 130 (2010) doi:10.1016/j.nuclphysb.2010.07.022 [arXiv:1006.1092 [hep-ph]].
 - [25] M. Kohda, H. Sugiyama and K. Tsumura, Phys. Lett. B **718**, 1436 (2013) doi:10.1016/j.physletb.2012.12.048 [arXiv:1210.5622 [hep-ph]].
 - [26] Y. Cai, J. D. Clarke, M. A. Schmidt and R. R. Volkas, JHEP **1502**, 161 (2015) doi:10.1007/JHEP02(2015)161 [arXiv:1410.0689 [hep-ph]].
 - [27] D. Aristizabal Sierra, A. Degee, L. Dorame and M. Hirsch, JHEP **1503**, 040 (2015) doi:10.1007/JHEP03(2015)040 [arXiv:1411.7038 [hep-ph]].
 - [28] J. C. Helo, M. Hirsch, T. Ota and F. A. P. d. Santos, JHEP **1505**, 092 (2015) doi:10.1007/JHEP05(2015)092 [arXiv:1502.05188 [hep-ph]].
 - [29] M. Hirsch, H. V. Klapdor-Kleingrothaus and S. G. Kovalenko, Phys. Rev. D **54**, 4207 (1996) doi:10.1103/PhysRevD.54.R4207 [hep-ph/9603213].
 - [30] K. m. Cheung, Phys. Rev. D **64**, 033001 (2001) doi:10.1103/PhysRevD.64.033001 [hep-ph/0102238].
 - [31] S. Baek and K. Nishiwaki, Phys. Rev. D **93**, no. 1, 015002 (2016) doi:10.1103/PhysRevD.93.015002 [arXiv:1509.07410 [hep-ph]].
 - [32] K. Cheung, W. Y. Keung and P. Y. Tseng, Phys. Rev. D **93**, no. 1, 015010 (2016) doi:10.1103/PhysRevD.93.015010 [arXiv:1508.01897 [hep-ph]].
 - [33] C. W. Murphy, arXiv:1512.06976 [hep-ph].
 - [34] I. Doršner, S. Fajfer, A. Greljo, J. F. Kamenik and

- N. Košnik, arXiv:1603.04993 [hep-ph].
- [35] M. Bauer and M. Neubert, arXiv:1512.06828 [hep-ph].
 - [36] C. D. Froggatt and H. B. Nielsen, Nucl. Phys. B **147**, 277 (1979). doi:10.1016/0550-3213(79)90316-X
 - [37] S. Davidson, D. C. Bailey and B. A. Campbell, Z. Phys. C **61**, 613 (1994) doi:10.1007/BF01552629 [hep-ph/9309310].
 - [38] ATLAS collaboration [ATLAS Collaboration], ATLAS-CONF-2015-081.
 - [39] CMS Collaboration [CMS Collaboration], collisions at 13TeV, CMS-PAS-EXO-15-004.
 - [40] J. P. Lees *et al.* [BaBar Collaboration], Phys. Rev. D **88**, no. 3, 031102 (2013) doi:10.1103/PhysRevD.88.031102 [arXiv:1207.0698 [hep-ex]].
 - [41] J. P. Lees *et al.* [BaBar Collaboration], Phys. Rev. D **86**, 012004 (2012) doi:10.1103/PhysRevD.86.012004 [arXiv:1204.2852 [hep-ex]].
 - [42] J. Adam *et al.* [MEG Collaboration], Phys. Rev. Lett. **110**, 201801 (2013) doi:10.1103/PhysRevLett.110.201801 [arXiv:1303.0754 [hep-ex]].
 - [43] A. E. C. Hernández, I. d. M. Varzielas and E. Schumacher, arXiv:1601.00661 [hep-ph].
 - [44] A. E. Cárcamo Hernández, I. de Medeiros Varzielas and E. Schumacher, Phys. Rev. D **93**, no. 1, 016003 (2016) doi:10.1103/PhysRevD.93.016003 [arXiv:1509.02083 [hep-ph]].
 - [45] A. E. C. Hernández, arXiv:1512.09092 [hep-ph].
 - [46] M. D. Campos, A. E. C. Hernández, H. Päs and E. Schumacher, Phys. Rev. D **91**, no. 11, 116011 (2015) doi:10.1103/PhysRevD.91.116011 [arXiv:1408.1652 [hep-ph]].
 - [47] N. Kosnik, Phys. Rev. D **86**, 055004 (2012) doi:10.1103/PhysRevD.86.055004 [arXiv:1206.2970 [hep-ph]].
 - [48] A. Leike, Phys. Rept. **317**, 143 (1999) doi:10.1016/S0370-1573(98)00133-1 [hep-ph/9805494].
 - [49] A. Djouadi, Phys. Rept. **459**, 1 (2008) doi:10.1016/j.physrep.2007.10.005 [hep-ph/0503173].
 - [50] A. D. Martin, W. J. Stirling, R. S. Thorne and G. Watt, Eur. Phys. J. C **63**, 189 (2009) doi:10.1140/epjc/s10052-009-1072-5 [arXiv:0901.0002 [hep-ph]].
 - [51] V. Khachatryan *et al.* [CMS Collaboration], Phys. Rev. D **91**, no. 5, 052009 (2015) doi:10.1103/PhysRevD.91.052009 [arXiv:1501.04198 [hep-ex]].
 - [52] G. Aad *et al.* [ATLAS Collaboration], Phys. Rev. D **91**, no. 5, 052007 (2015) doi:10.1103/PhysRevD.91.052007 [arXiv:1407.1376 [hep-ex]].
 - [53] R. Franceschini *et al.*, arXiv:1512.04933 [hep-ph].